10.2478/msr-2014-0007

MEASUREMENT SCIENCE REVIEW, Volume 14, No. 1, 2014

# CMF Signal Processing Method Based on Feedback Corrected ANF and Hilbert Transformation

Yaqing Tu, Huiyue Yang, Haitao Zhang, Xiangyu Liu

Logistical Engineering University, Chongqing 401311, P.R.C
E-mail address:yq.tu@163.com; huiyue_yang@163.com

**In this paper, we focus on CMF signal processing and aim to resolve the problems of precision sharp-decline occurrence when using adaptive notch filters (ANFs) for tracking the signal frequency for a long time and phase difference calculation depending on frequency by the sliding Goertzel algorithm (SGA) or the recursive DTFT algorithm with negative frequency contribution. A novel method is proposed based on feedback corrected ANF and Hilbert transformation. We design an index to evaluate whether the ANF loses the signal frequency or not, according to the correlation between the output and input signals. If the signal frequency is lost, the ANF parameters will be adjusted duly. At the same time, singular value decomposition (SVD) algorithm is introduced to reduce noise. And then, phase difference between the two signals is detected through trigonometry and Hilbert transformation. With the frequency and phase difference obtained, time interval of the two signals is calculated. Accordingly, the mass flow rate is derived. Simulation and experimental results show that the proposed method always preserves a constant high precision of frequency tracking and a better performance of phase difference measurement compared with the SGA or the recursive DTFT algorithm with negative frequency contribution.**

**Keywords: Coriolis mass flow meter, adaptive notch filter, Hilbert transform, frequency track, phase difference.**

## 1. INTRODUCTION

DURING THE last decades, interest in Coriolis mass flow meters (CMFs) has been increasing steadily. A reason is that CMFs directly measure the mass flow, whereas other instruments measure volumetric flow [1]. High precision, wide tolerance of measurable fluids and multi-parameter measurement also justify their fast growth and acceptance in industry. Mass flow rate is obtained in CMF by measuring the time interval, which is dependent on the frequency and the phase difference between two vibration signals detected by electromagnetic sensors. Therefore, the precise measurements of the signal frequency and the phase difference are the cores of CMF signal processing.

Traditional analogue methods for CMF signal processing are of poor interference resistance and measured results are phase differences of resultant waves [2]. Various digital methods have been recently introduced into CMF so as to improve the precision [3]. Romano [4] introduced the discrete Fourier transform (DFT) into CMF signal processing for the first time in 1990. The signal frequency was calculated by DFT, and the phase difference was obtained by subtracting two DFT phases at the maximum spectral line. This method is of good resistance to harmonic interference but calls for an unfeasible technique of integral period sampling which limits its practicality. Freeman and Ashevillc [5] adopted digital phase-locked loop (PLL) to track the vibrating frequency of flow tubes. Denis [6] presented a method for CMF signal processing based on orthogonal demodulation. However, precision of the method depended on the performance of low-pass filters.

A sliding Goertzel algorithm (SGA) was introduced to measure the phase difference between CMF signals. The SGA generates phase difference continuously, but there is a slow convergence rate and a numerical overflow. What is more, the SGA needs frequency when the phase difference is calculated. In [8], a method was proposed for CMF signal processing based on recursive DTFT algorithm with negative frequency contribution. When the Fourier coefficients are calculated, the method accelerates the convergence rate and improves the accuracy greatly. But the signal frequency is also needed.

In [9], adaptive notch filter (ANF) was introduced to CMF signal frequency tracking. The ANF's structural parameters were adjusted automatically according to signal characteristics and the vibrating frequency of flow tubes is generated continually. Thanks to the frequency tracking ability and good resistance to noise, the ANF has gained a lot of attention recently. A lattice ANF (LANF) was brought in CMF signal processing in [10]. [11] and [12] introduced a novel IIR-type ANF evolved from the Steiglitz-McBride method (SMM-ANF) [13] for CMF signal frequency tracking. The novel ANF has unbiased theory results, high precision and faster convergence rate compared with LANF. However, these ANFs including the novel ANF cannot supply constantly high-accuracy results. It has limited their applications in CMF signal processing.

To improve the precision of CMFs, a new method is proposed in this paper based on feedback corrected ANF and Hilbert transformation [14]. The method is expected to supply constantly high-accuracy results and eliminate the dependence on frequency when calculating phase difference.

This paper is organized into six sections. Section 2 introduces the proposed method process. In Section 3, a feedback corrected ANF is proposed for frequency estimation. Section 4 presents a phase difference measurement method based on the Hilbert transformation. The proposed method for signal frequency estimation and phase difference measurement is validated by simulations and experiments in Section 5 and Section 6, respectively. Conclusions are drawn in the last section.

## 2. METHOD PROCESS

Process of the proposed method is expounded in Fig.1., from which we can see that the frequency estimation and the phase difference measurement are carried out in parallel, differing from the existing methods. On the one hand, SVD algorithm is firstly used to reduce the noise contained in CMF signals. And then phase difference is calculated by trigonometry operation between the noise-reduced signals and those after the Hilbert transformation. On the other hand, signal frequency is estimated continually by the feedback corrected SMM-based ANF. Then, time interval of the two signals is figured out as the frequency and the phase difference is obtained. Accordingly, the mass flow rate is derived.

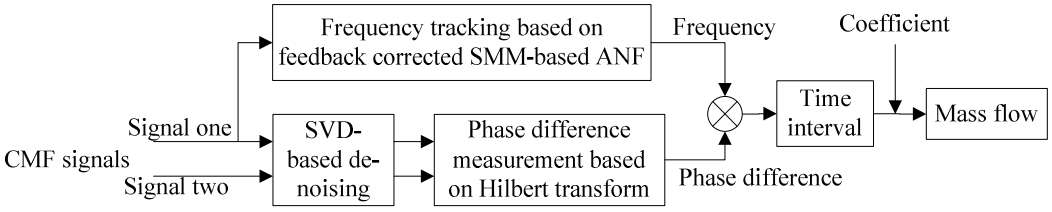


Fig.1. The signal processing flow chart.

## 3. FREQUENCY ESTIMATION BASED ON FEEDBACK CORRECTED ANF

A strategy of feedback correction for ANF is proposed so as to improve the stability of its accuracy. According to the correlativity between the output and input signals, we design an index for real-time evaluation of the frequency estimation precision. If the index overruns its limit, ANF parameters will be adjusted adhering to the feedback. The SMM-ANF is taken as an examination for the feasibility of the proposed strategy.

### *A. The SMM-ANF*

Structure of the ANF based on Steiglitz-McBride method is shown in Fig.2, and its transfer function is given by:

$$H(z)=\frac{\hat{A}_n(z^{-1})}{\hat{A}_n(\rho z^{-1})}=\prod_{k=1}^{m}\frac{1+\hat{\alpha}_k(n)z^{-1}+z^{-2}}{1+\rho_k\hat{\alpha}_k(n)z^{-1}+\rho_k^2 z^{-2}} \qquad (1)$$

Where

$m$ is the trap number, namely the sine wave number in $y(n)$;

$\rho_k$ is pole contraction factor determining the trap bandwidth

$\Delta$ is used to reduce the correlation between the noise in $y(n)$ and $y(n-\Delta)$, $\Delta \geq 1$.

$\hat{\alpha}_k(n)$ is adaptive adjusted through the Newton-type algorithm, $\hat{\alpha}_k(n)=-2\cos\hat{\omega}_k(n)$, $\hat{\omega}_k(n)$ is notch frequency corresponding to the sinusoidal frequency.

A 2-order ANF with a single trap is used in our study as the CMF signals have only one expectant sinusoidal.

The ANF bandwidth is often initialized with a big value and then decreases step by step so as to acquire the signal frequency.

$$BW=2\cos^{-1}\left(\frac{2\rho(t)}{1+\rho^2(t)}\right) \qquad (2)$$

At convergent stage, the pole contraction factor comes to one and the bandwidth approximately equals to zero (2). However, due to the ANF inherent structure, there is an incomplete convergence stage especially when the signal frequency is very low or very high (close to Nyquist frequency). At this stage, the ANF's non-quadratic error rests on a local minimum, and then the signal frequency will be lost soon.

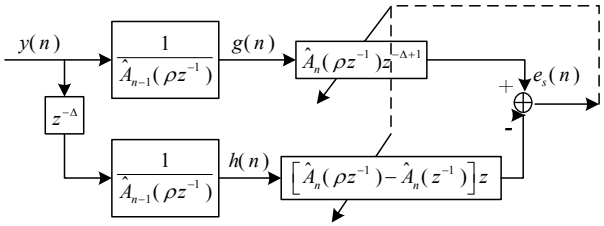


Fig.2. Structure of the SMM-ANF

### *B. Assessment of frequency estimation accuracy*

The noise-reduced signal $\hat{c}(n)$ shown in Fig.3. is obtained by the output $e_s(n)$ and the input $y(n)$, expressed as

$$\hat{c}(n)=\frac{(\rho-1)\hat{\alpha}(n)z^{-1}+(\rho^2-1)z^{-2}}{1+\rho\hat{\alpha}(n)z^{-1}+\rho^2 z^{-2}}y(n) \qquad (3)$$

Thanks to the independence of noise or $y(n-\Delta n)$, the signal $\hat{c}(n)$ approximates to $c(n)$ when the ANF works well. Otherwise, the signal $\hat{c}(n)$ approximates to $e(n)$. Consequently, index $h$ is designed to evaluate the accuracy of the ANF. The index is calculated online in real time by the 0-order LMS, as follows:

$$\begin{cases}\varepsilon(n)=\hat{c}(n)-h(n)y(n)\\ h(n)=h(n-1)+\mu_h\varepsilon(n)y(n)\end{cases} \qquad (4)$$

where, $\mu_h$ is the step size, and $h$ is the solution of Wiener-Hopf equation on the convergence condition.

$$h \cdot E\left\{y^2(n)\right\} = E\left\{y(n)\hat{c}(n)\right\} \tag{5}$$

$E\{c(n)e(n)\}$ equals to zero as the signal $c(n)$ is unrelated to noise $e(n)$. Then, the (5) can be written:

$$h \cdot \left(E\left\{c^2(n)\right\} + E\left\{e^2(n)]\right\}\right) = E\left\{c(n)\hat{c}(n)\right\} + E\left\{e(n)\right\} E\left\{\hat{c}(n)\right\} \tag{6}$$

With $E\{e(n)\}$, $E\{e^2(n)\}$ and $E\{c^2(n)\}$ equal to 0, $\sigma_e^2$ and $A^2/2$, respectively, the index $h$ can be derived as:

$$h = \frac{E\left\{c(n)\hat{c}(n)\right\}}{A^2/2 + \sigma_e^2} \tag{7}$$

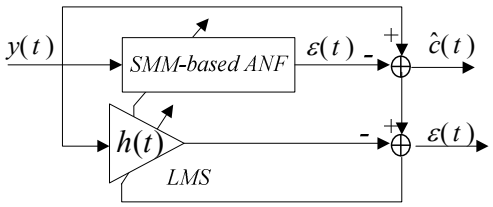


Fig.3. Structure of the feedback modified SMM-ANF.

There are two possible situations for the index $h$ with either good or bad performance of the ANF.

• If the ANF works well, $\hat{c}(n)$ approximates to $c(n)$ and then, the index $h = A^2/(A^2 + 2\sigma_e^2)$.

• If the ANF loses the signal frequency, there is no correlation between $\hat{c}(n)$ and $c(n)$. Therefore, the expected value $E\{c(n)\hat{c}(n)\}$ can approximate to zero, and then, the index $h$ comes to zero consequently.

### C. Feedback correction strategy

A comparative parameter $T_h$ is initialized with small value so as to judge whether the ANF loses the signal frequency or not. If $h$ is greater than $T_h$, we have nothing to do. Otherwise, the ANF's parameters will be adjusted according to a random search method, rather than simply re-initialization, which will lead to another convergence process. The correction strategy of the two key parameters $\lambda$ and $\rho$ of the SMM- ANF is given by

$$\begin{cases} \lambda(n) = \lambda_\infty + \delta_\lambda \ , \ 0 < \delta_\lambda < \lambda_\infty - \lambda(0) \\ \rho(n) = \lambda_\infty + \delta_\rho \ , \ 0 < \rho_\lambda < \rho_\infty - \rho(0) \end{cases} \tag{8}$$

where $\lambda_\infty$ and $\rho_\infty$ denote the final value of $\lambda$ and $\rho$, respectively, $\delta_\lambda$ and $\delta_\rho$ are the step size.

## 4. Phase difference measurement based on Hilbert transformation

A phase difference measurement method based on the Hilbert transformation is proposed in this section, expecting to eliminate the dependence on signal frequency. The singular value decomposition (SVD) algorithm is firstly used to reduce the noises in CMF signal. Then, the phase difference is calculated using the $\pm\pi/2$ phase-shift property of the Hilbert transformation.

### A. SVD-based noise reduction

There is a $m$-order orthogonal matrix $\mathbf{U}$ called the left singular value vector and a $n$-order orthogonal matrix $\mathbf{V}$ called the right singular value vector. The two matrices satisfy the equation that $\Sigma = \mathbf{U}^{\mathbf{T}}\mathbf{A}\mathbf{V}$ .Where,

$\mathbf{A}$ is the Hank matrix composed of signal $x(t)$, specified in (13)

$\Sigma$ is a $\mathbf{M} \times \mathbf{N}$ non-negative diagonal matrix with $\sigma_1 \geq \sigma_2 \geq \cdots \geq \sigma_N \geq 0$ on its diagonal positions.

$\sigma_i (1 \leq i \leq N)$ are the singular values representing the energy of matrix $\mathbf{A}$.

Noise-reduced signal can be constructed by reserving the fore $r$ singular values which correspond to signal power and setting the others zero which define the noise components.

$$\mathbf{A} = \begin{bmatrix} x(1) & x(2) & \ldots\ldots & x(n) \\ x(2) & x(3) & \ldots\ldots & x(n+1) \\ \vdots & \vdots & \vdots & \vdots \\ x(N-m+1) & x(N-m+2) & \ldots\ldots & x(N) \end{bmatrix} \tag{9}$$

The rank $r$ is the key for the best separation of the signal and noises. To choose an optimal rank $r$, singular entropy is defined as

$$E_r = \sum_{i=1}^{r} \Delta E_r \tag{10}$$

where $\Delta E_i$ is the singular entropy increment at the rank $i$, computed by

$$\Delta E_i = -\left(\sigma_i / \sum r\right) \ln\left(\sigma_i / \sum_{r=1}^{m} \sigma_i\right) \tag{11}$$

The singular entropy $E_r$, which reflects the information contained in the signal, increases rapidly when the rank is low. The increase of $E_r$ drops off with the rise of rank, as the signal component contribution arrives at the maximum. Then, the rank $i$ can guarantee a good denoising performance.

The SVD-based noise reduction algorithm is simple in principle, easy to implement, but only useful to stationary signals. Therefore, a sliding rectangular window is adopted to cut the CMF signal into steady overlap segments.

### B. Phase difference calculation

Hilbert transformation enjoys a $\pm\pi/2$ phase-shift property. Hereby, the phase difference function can be derived by the trigonometric operator between the CMF signal and its Hilbert transformation.

CMF signals detected by electromagnetic sensors can be described by

$$\begin{aligned} y_1(n) &= A(n)\sin(\omega(n)+\varphi_1(n))+\sigma_e\cdot e_1(n) \\ y_2(n) &= A(n)\sin(\omega(n)+\varphi_2(n))+\sigma_e\cdot e_2(n) \end{aligned} \quad (12)$$

where, $A(n)$ is the amplitude, $\varphi_1(n)$ and $\varphi_2(n)$ are initial phases; $\omega(n)$ is the singular frequency, $\omega = 2\pi f / f_s$.

Our goal is to evaluate the phase difference $\Delta\varphi(n)$, $\Delta\varphi(n) = \varphi_1(n) - \varphi_2(n)$. The Hilbert transformations of the two CMF signals are given by

$$\begin{aligned} \hat{y}_1(n) &= -A(n)\cos(\omega(n)+\varphi_1(n))+\sigma_e\cdot e_3(n) \\ \hat{y}_2(n) &= -A(n)\cos(\omega(n)+\varphi_2(n))+\sigma_e\cdot e_4(n) \end{aligned} \quad (13)$$

The phase difference $\Delta\varphi(n)$ can be derived:

$$\Delta\varphi(n) = arc\tan\left(\frac{\hat{y}_1(n)y_2(n)-\hat{y}_2(n)y_1(n)}{y_1(n)y_2(n)+\hat{y}_1(n)\hat{y}_2(n)}\right) \quad (14)$$

Then, phase difference is measured at every sampling point in time region, despite the signal frequency [14].

## 5. Simulation results

Computer simulations and actual experiments have been done to evaluate the proposed method. Their results are presented in the following sections, respectively.

### A. Simulated signals

The CMF signal parameters vary from time to time due to the effect of fluid properties, flow pulsation, etc. A time-varying signal model, in which the signal frequency, amplitude, and phase vary over time based on the random walk model, was presented in [15] so as to more closely describe the CMF signals. However, this model failed to describe the signals in special conditions such as pulsating flows. Hereby, the time-varying signal model based on random walk is amended, as follows:

$$y(n) = A(n)\sin[\omega(n)+\phi(n)]+\sigma_e\cdot e(n) \quad (15)$$

$$A(n) = A(n-1)+\delta_A\cdot\sigma_A\cdot e_A(n) \quad (16)$$

$$\omega(n) = \omega(n-1)+\delta_\omega\cdot\sigma_\omega\cdot e_\omega(n) \quad (17)$$

$$\phi(n) = \phi(n-1)+\delta_\phi\cdot\sigma_\phi\cdot e_\phi(n) \quad (18)$$

where, $e(n)$, $e_A(n)$, $e_\omega(n)$, and $e_\phi(n)$ are white noises, with no correlation between each other. $\sigma_e$, $\sigma_A$, $\sigma_\omega$ and $\sigma_\phi$ are the walk amplifications, while $\delta_A$, $\delta_\omega$ and $\delta_\phi$ are walk factors following 0-1 distribution with the probabilities $P_A$, $P_\omega$ and $P_\varphi$ respectively. The probabilities are determined by the flow character and environment.

Table 1. Initializations of simulation parameters.

| Name | Initial value | Name | Initial value |
|---|---|---|---|
| Amplitude | $A(0)=10$ mV | Probabilities | $P_A = P_\omega = P_\varphi = 0.5$ |
| Frequency | $f = 198$ Hz | Sample frequency | $f_s = 2000$ Hz |
| Step size | $\sigma_e = 0.6$, $\sigma_A = 10^{-3}$, $\sigma_\omega = 10^{-6}$, $\sigma_\varphi = 10^{-3}$ | | |

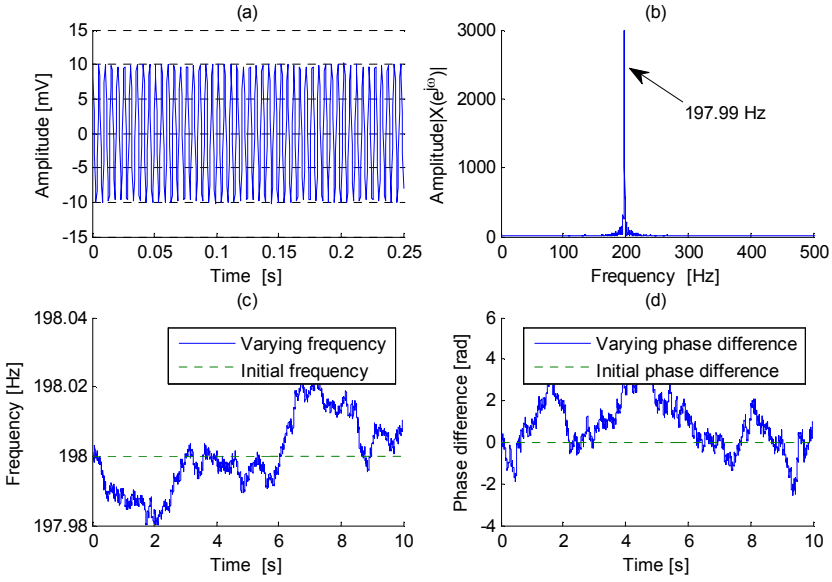


Fig.4. Simulated signals.

When the probabilities approximately equal to zero, the amended time-varying signal model degenerates to the sinusoidal with superposed white noise, describing the CMF signal under the circumstance of steady flow. When the probabilities come to one, it is the original time-varying model, describing the CMF signal under the circumstance of general fluctuant flow. The CMF signals under the circumstance of mutation flow can also be described by reducing the probabilities and increasing the walk amplification.

Signals used in simulations are generated according to the time-varying signal model amended above. Parameters of the signal model are initialized as Table 1. Fig.4. shows the simulated signal, the frequency spectrum, the varying frequency and the varying phase difference.

### *B. Frequency estimation results*

The signal frequency is estimated by the feedback corrected SMM-ANF, while the lattice ANF and the original SMM-ANF are used as control experiments. The results are shown in Fig.5. It can be concluded from the results that the feedback corrected SMM-ANF converges faster than the LANF, slightly slower than the original SMM-ANF. The feedback corrected SMM-ANF has a higher precision compared with the LANF and the original SMM-ANF, especially when they work for a long time. The reason is that the feedback corrected SMM-ANF utilizes a designed index for observing the accuracy continuously and adjusts its own non-effective parameters duly.

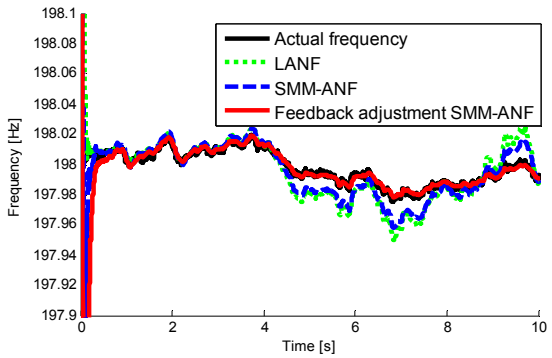


Fig.5. Performances of frequency tracking.

To describe the precision advantage of the feedback corrected SMM-ANF in detail, Monte Carlo simulations have been done for 100 times independently and the mean square errors (MSEs) were calculated by

$$MSE = \frac{1}{N - m}\sum_{i=m}^{N}\left[\hat{f}(i) - f(i)\right]^2 \qquad (19)$$

where $f(i)$ and $\hat{f}(i)$ are the actual frequency and the estimated frequency, respectively. $m$ is the beginning of the computing signal, while $N$ is the end. The estimated frequency in the convergence process has not been compared in this research so as to guarantee the justice. $m$ equals to 4,000, and $N$ is 40,000, the length of the simulated signal.

Fig.6. shows the MSEs of frequency estimation. From Fig.6., it can be seen that the MSEs of the feedback corrected SMM-ANF are the steadiest and the lowest, compared with the LANF and the SMM-ANF. The MSEs mean of the feedback corrected SMM-ANF is 0.26 % of the LANF, 1.58 % of the original SMM-ANF.

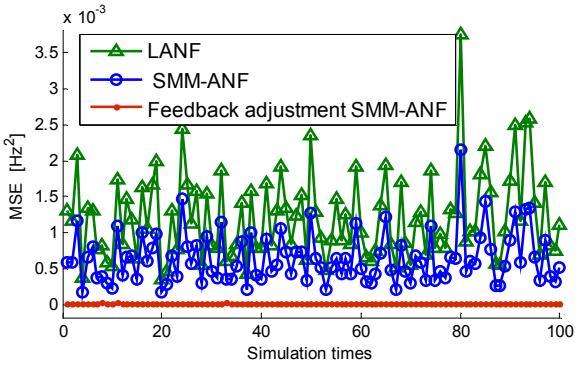


Fig.6. MSEs of frequency estimation.

### *C. Phase difference measurement results*

The properties of the proposed phase difference measurement method are analyzed with the SGA and the recursive DTFT algorithm with negative frequency contribution (the algorithm in [8] for short) as comparisons. The phase difference measurement results are presented in Fig.7.

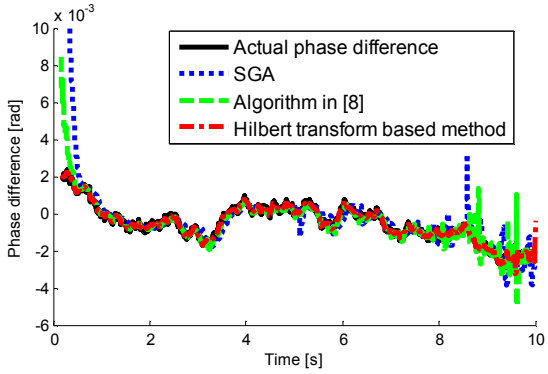


Fig.7. Performance of phase difference measurement.

It can be seen from Fig.7. that the proposed method based on the Hilbert transformation has no convergence process and outputs the results from the beginning, while the SGA and the algorithm in [8] need a time to converge. The reason of this phenomenon is that the proposed method needs no iterations and calculates the phase difference through the trigonometry operator between the original CMF signals and those after their Hilbert transformations, very different from the SGA and the algorithm in [8] depending on DFT iterative calculation. Observing the local results of phase difference measurement, we can also see that the SGA has a time delay and cannot reflect the details. This is due to the requirement for a long sliding window in the SGA (400 points in the experiment with 350 points overlapped). With the negative frequency contribution being considered, the

algorithm in [8] can detect a small phase difference change with a very short window (8 points in this experiment with 7 points overlapped). The ability of dynamic phase difference measurement is also significantly improved. As for the proposed method based on the Hilbert transformation, the phase difference is directly calculated by the CMF signals and those after their Hilbert transformation, with no DFT. Accordingly, there are no subsections and no iteration operations in the proposed method. Therefore, the dynamic measuring performance is further improved.

## 6. Experimental Results and Discussion

### A. Experimental system

As shown in Fig.8., the experimental system for CMF signal processing consists of two CMFs (F200S with a 1700R transmitter, and TQ-884 with an ERE10 transmitter), a PLC used to change flow, a pump, a batch tank and a signal acquisition subsystem. The signal acquisition subsystem consists of two data acquisition devices (NI 9234 and USB4711), an electric scale (FS3198-2), and a computer.

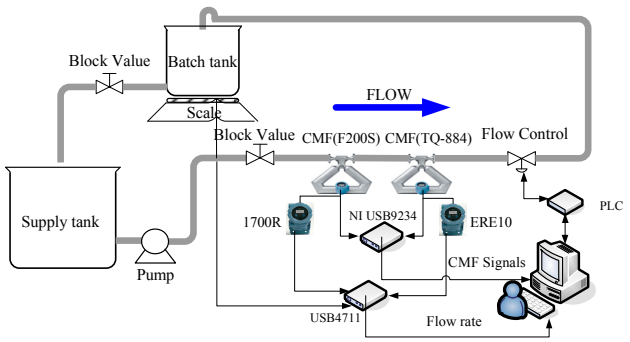


Fig.8. Block of the experimental system.

Flow rate is controlled by computer through the PLC and a control valve. CMF oscillation signals are acquired by the 4-channel dynamic signal acquisition NI 9234. Instantaneous mass flow rate measured by the CMFs is collected by the USB4711. Mass flow measured by the scale is deemed as the actual value. The test of the proposed signal processing method is carried out by the computer. The oscillation signals used in the experiments come from the F200S CMF with its higher precision and stable performance compared with the TQ-884 CMF.

### B. Results

According to CMF's principle, there is a linear relationship between the mass flow rate $q_m$ and the time interval $\Delta t$, that is

$$q_m = k \cdot \Delta t + b \tag{20}$$

Where, the parameter $b$ is constant. The time interval $\Delta t$ depends on the frequency and the phase difference. The coefficient $k$ is decided by the CMF type, temperature, pressure and so on, but is fixed at the same situation. For the F200S CMF, we were informed of $k = 19.3534$ and $b = 1.0471$ from the manufacturers.

Display values of F200S CMF are deemed as actual mass flow. The SGA and the algorithm in [8] are taken as comparisons. As we know, the SGA and the algorithm in [8] need signal frequency to conclude the phase difference. To guarantee the justice, frequency estimated by the feedback corrected SMM-ANF is used identically. Signals at nine kinds of steady flow are collected and processed. Mass flow is computed and shown in Table 2. It can be seen that the results concluded by the three methods agree with each other. The proposed method owns the highest precision, whose relative error is below 0.5 %. Then, we come to the conclusion that the proposed method is effective and practical.

Table 2. Experimental results.

| Mass flow (kg/min) | Estimated frequency(Hz) | SGA (kg/min) | Algorithm in[8] (kg/min) | The proposed method (kg/min) |
|---|---|---|---|---|
| 2.9700 | 198.4483 | 3.0275 | 2.9151 | 2.9368 |
| 10.0400 | 198.3953 | 10.1910 | 10.1612 | 10.1364 |
| 15.9800 | 198.3863 | 15.8070 | 15.8294 | 16.1212 |
| 29.9100 | 198.3946 | 30.2341 | 30.2142 | 29.6848 |
| 41.2800 | 198.4299 | 41.5911 | 41.0279 | 41.1027 |
| 63.4500 | 198.3927 | 63.8731 | 63.7980 | 63.1618 |
| 82.1300 | 198.3993 | 81.6201 | 82.5802 | 82.4763 |
| 98.7600 | 198.4109 | 98.0135 | 99.2973 | 99.1905 |
| 102.2800 | 198.4075 | 102.9942 | 101.5669 | 102.6956 |
| 132.6100 | 198.4136 | 133.5964 | 133.5016 | 132.0320 |

## 7. Conclusion

The core of CMF signal processing is the frequency estimation and the phase difference measurement. However, there is a dependence on frequency when the SGA or the algorithm in [8] is used to calculate the phase difference. It is a requirement that the signal frequency is timely tracked with a high-precision, due to its time-varying character. A comprehensive novel method for CMF signal processing is proposed based on the feedback corrected SMM-ANF and the Hilbert transformation. Simulation and experimental results validate the proposed method and indicate some of its advantages, including:

• The proposed method carries out frequency tracking and phase difference measurement independently. We can obtain the frequency and the phase difference at the same time. Thus, the ability of real-time measurement is improved accordingly.

• For frequency tracking, the presented feedback corrected SMM-ANF enjoys a constantly high accuracy, while others undergo a sharp decline in accuracy when working for a long time. The MSE's mean of the feedback corrected SMM-ANF is 0.26 % of the LANF, 1.58 % of the original SMM-ANF. What is more, the strategy of the feedback correction is also applicable for other ANFs.

• For phase difference measurement, the presented method based on the Hilbert transformation calculates the results directly, with no iterative operation and no convergence stage, and performs better in accuracy, compared with the SGA and the algorithm in [8].

To improve the precision and shorten the calculation time of the CMF signal processing, this paper suggests carrying out the frequency tracking and the phase difference measurement independently. The idea has preliminarily been validated by the methods proposed in Section 3 and Section 4, and further research is under discussion.

## ACKNOWLEDGMENT

This work is supported by National Natural Science Foundation of China (61271449, 61302175), and Natural Science Foundation of Chongqing, China (CSTC, 2011BA2015, cstc2013jcyjA40030).

## REFERENCES

[1] Shanmugavalli, M., Umapathy, M., Uma, G. (2010). Smart Coriolis mass flowmeter. *Measurement,* 43 (4), 549-555.

[2] Matt, Ch. (2010). *Method for determining the mass flow through a coriolis mass flowmeter*. United States Patent 7854176.

[3] Kitami, H., Shimada, H. (2011). *Signal processing method, signal processing apparatus, and coriolis flowmeter*. United States Patent 0203389.

[4] Romano, P. (1990). *Coriolis mass flow rate meter having a substrantially increased noise immunity*. United States Patent 4934196.

[5] Freeman, B.S. (1998). *Digital phase locked loop signal processing for coriolis mass flow meter*. United States Patent 5804741.

[6] Henrot, D. (2001). *Multi-rate digital signal processor for vibrating conduit sensor signals*. WIPO Patent 0101083.

[7] Xu, K.-J., Xu, W.-F. (2007). A signal processing method based on AFF and SGA for coriolis mass flowmeters. *Acta Metrologica Sinica*, 28 (1), 48-51.

[8] Tu, Y., Zhang, H. (2008). Method for CMF signal processing based on the recursive DTFT algorithm with negative frequency contribution. *IEEE Transactions on Instrumentation and Measurement*, 57 (11), 2647-2653.

[9] Bose, T, Derby, H.V., Rajan, S. (1996). *Method and apparatus for adaptive line enhancement in Coriolis mass flow meter measurement*. United States Patent 5555190.

[10] Xu, K.-J., Ni, W. (2005). A lattice notch filter based signal processing method for coriolis mass flowmeter. *Acta Metrologica Sinica*, 26 (1), 49-52.

[11] Tu, Y.-Q., Su, F.-H., Shen, T.-A., Zhang, H.-T. (2011). New adaptive notch filter based a time-varying frequency tracking method and simulation for coriolis mass flowmeter. *Journal of Chongqing University*, 34 (10), 147-152.

[12] Yang, H., Tu, Y., Zhang, H. (2012). A frequency tracking method based on improved adaptive notch filter for coriolis mass flowmeter. *Applied Mechanics and Materials*, 128-129, 450-456.

[13] Cheng, M.-H., Tsai, J.-L. (2006). A new IIR adaptive notch filter. *Signal Processing*, 86 (7), 1648-1655.

[14] Vucijak, N.M., Saranovac, L.V. (2010). A simple algorithm for the estimation of phase difference between two sinusoidal voltages. *IEEE Transactions on Instrumentation and Measurement*, 59 (12), 3152-3158.

[15] Li, Y., Xu, K., Zhu, Z., Hou, Q. (2010). Study and implementation of processing method for time-varying signal of eoriolis mass flowmeter. *Chinese Journal of Scientific Instrument*, 1, 8-14.

Received April 26, 2013.
Accepted February 6, 2014.